

Superconductivity induced by inter-band nesting in the three-dimensional honeycomb lattice

Seiichiro Onari, Kazuhiko Kuroki¹, Ryotaro Arita, and Hideo Aoki

Department of Physics, University of Tokyo, Hongo, Tokyo 113-0033, Japan

¹*Department of Applied Physics and Chemistry, University of Electro-Communications, Chofu, Tokyo 182-8585, Japan*

(December 2, 2024)

In order to study whether the inter-band nesting can favor superconductivity arising from electron-electron repulsion in a three-dimensional system, we have looked at the repulsive Hubbard model on a stack of honeycomb (i.e., a non-Bravais) lattices with the FLEX method, partly motivated by the superconductivity observed in MgB_2 and graphite intercalation compounds. By systematically changing the shape of Fermi surface with varied band filling n and the third-direction hopping, the inter-band nesting is indeed found to give rise to gap functions that change sign across the bands and behave as s- or d-wave within each band. This implies (a) the electron repulsion can assist a *gapful* pairing when the phonon-mechanism pairing exists, and (b) the electron repulsion alone, when strong enough, can give rise to a d-wave-like pairing, which should be, for a group-theoretic reason, a time-reversal broken d+id with *point nodes* in the gap.

PACS numbers: 74.20.Mn

I. INTRODUCTION

Recent discovery of the superconductivity in MgB_2 ¹ with relatively high transition temperature ($T_c \sim 39\text{K}$) has invoked renewed interests in *sp*-bonded materials. Electronically, the system is a π electron system on layered honeycomb lattice, which immediately reminds us of graphite intercalation compounds (GIC) such as LiC_6 ² or KC_8 ^{3,4}.

While the GIC is considered to be a conventional superconductor with $T_c < 5\text{K}$, MgB_2 has an unusually high T_c found in *sp*-bonded materials (with a recent exception of C_{60} -FET structure⁵). Recently, Choi *et al.*⁶ have used the ab-initio pseudopotential density functional theory to solve Eliashberg's equation numerically, and have reproduced $T_c \sim 39\text{K}$, isotope-effect exponent $\alpha_B \sim 0.3$ ^{7,8}, and have obtained the gapful BCS pairing, which is consistent with experimental results such as specific heat^{9,10}, tunneling and photoemission spectra^{11–14}, penetration depth¹⁵, and the Raman spectra¹⁶. Thus both GIC and MgB_2 seem to be mainly phonon-mediated superconductors. However, to realize high T_c 's, electron repulsion should not stand in the way of the phonon mechanism, so the question on one hand may be paraphrased: can the electron repulsion avoid destroying or possibly even assist the phonon-mediated pairing.

On the other hand, superconductivity from electron-electron repulsion itself is fascinating in many ways, but there are many open questions. While there is a growing consensus that high- T_c cuprates may be related to the electron correlation, we are only beginning to understand the link between the underlying band structure and the way in which the electron-mechanism superconductivity appears¹⁷. The way in which this occurs can be sensitively affected by the shape of the Fermi surface. Recently, two of the present authors proposed¹⁸

that multi-band systems should open a new possibility of much higher T_c , where a fully gapped BCS gap function can appear when the Fermi surface consists of disconnected pieces, while the usual wisdom dictates that the repulsion-originated superconductivity should have, as in the cuprates, a strongly anisotropic gap function with nodes. They have conceived and demonstrated this for some two-dimensional lattice models. The physics is that inter-Fermi-surface-pocket pair scattering processes can give rise to a gap function who changes sign across the pockets, but has the same sign within each pocket.

So the purpose of the present paper is a combination of the above two motivations. Namely, we study whether the inter-band nesting can favor superconductivity arising from electron repulsion in a three-dimensional system, by taking the repulsive Hubbard model on a stack of honeycomb lattices as a prototype. There, the honeycomb, a typical non-Bravais lattice, provides two bands, while the stacking can provide a natural nesting along that direction. So, if the scattering of pairs in a band across to pairs in another around this nesting vector works favorably, we can expect a pairing from the interband nesting.

So we have studied the systematic dependence of the solution of Eliashberg's equation with the multi-band fluctuation exchange approximation on the shape of Fermi surface by changing the band filling and the third-direction hopping. The presence of a strong inter-band nesting is found to indeed give rise to inter-band gap functions that change sign across the two bands, but, more precisely there exist two, nearly degenerate modes that behave respectively like s- and d-waves within each band. This implies (a) the electron repulsion can assist an s-wave like pairing when the phonon-mechanism pairing exists as a dominant mechanism. We have further found that (b) when the electron repulsion is strong

enough, the d-wave is realized, which should be, for a group-theoretic reason, a time-reversal broken linear combination of two symmetries with *point* nodes in the gap.

According to the band calculation¹⁹, the Fermi surface of MgB₂ consists of two tubular networks having a boron-2p π character along with two cylinders of the boron-2p σ characters. As has been stressed by several authors^{20,21}, the nesting between these two π bands are quite good. Thus taking the stacked honeycomb lattice does indeed suit our purpose. Although $p\sigma$ bands are considered to be important in that the electron-phonon interaction is much stronger in this band, here we concentrate on the $p\pi$ bands in order to focus on the effects of the Fermi surface nesting. The GIC, on the other hand, has a much smaller inter-layer transfer energy (t_z), so that the Fermi surface is a cylinder of carbon π character with no dominant nesting vectors. So in the latter part of the paper we shall cover both MgB₂- and GIC-situations in a systematic variation of t_z and band filling. The systematic study also serves to explore how the inter- and intra-band nesting compete in realizing superconductivity.

II. FORMULATION

Now let us start with the case corresponding to MgB₂. Spin-fluctuation-mediated superconductivity is here studied with the fluctuation exchange approximation (FLEX) developed by Bickers *et al.*^{22–25}. The model is a 3D two-band Hubbard model with the repulsion U on layered honeycomb lattice,

$$\mathcal{H} = \sum_{\langle i,j \rangle, \sigma} \sum_{\alpha, \beta}^{A, B} t_{ij} \left(c_{i\sigma}^{\alpha\dagger} c_{j\sigma}^{\beta} + \text{H.c.} \right) + U \sum_i \sum_{\alpha} n_{i\uparrow}^{\alpha} n_{i\downarrow}^{\alpha}, \quad (1)$$

in standard notations. The essential ingredient is the non-Bravais lattice, which has two bands within a layer. Here we assume a non-staggered layer stacking as realized in MgB₂ and GIC (Fig.1), which also depicts the inter-layer hopping t_z . Hereafter we take the intra-layer hopping $t = -1$.

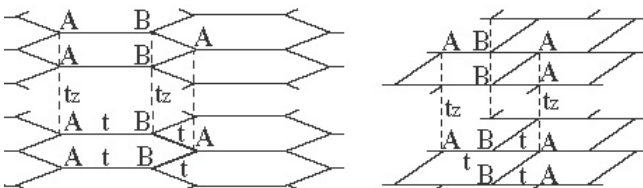


FIG. 1. 3D layered honeycomb lattice (the left panel), which is topologically equivalent to the lattice in the right panel. A and B indicate sublattices.

The noninteracting band dispersion for 3D honeycomb is,

$$\epsilon(\mathbf{k}) = 2t_z \cos k_z \pm t \sqrt{3 + 2 [\cos k_x + \cos k_y + \cos(k_x + k_y)]}. \quad (2)$$

In the two-band FLEX^{26,27}, Green's function G , self-energy Σ , susceptibility χ , and the gap function ϕ all become 2×2 matrices, such as $G_{\alpha\beta}(k)$, where $k \equiv (\mathbf{k}, i\omega_n)$ with $\omega_n = (2n-1)\pi T$ being the Matsubara frequency for fermions.

The self-energy is given by

$$\Sigma_{\alpha\beta}^{(1)}(k) = \frac{T}{N} \sum_q G_{\alpha\beta}(k-q) V_{\alpha\beta}^{(1)}(q), \quad (3)$$

where the fluctuation-exchange interaction $V^{(1)}(q)$ is

$$V_{\alpha\beta}^{(1)}(q) = \frac{3}{2} U^2 \left[\frac{\chi^{\text{irr}}(q)}{1 - U\chi^{\text{irr}}(q)} \right]_{\alpha\beta} + \frac{1}{2} U^2 \left[\frac{\chi^{\text{irr}}(q)}{1 + U\chi^{\text{irr}}(q)} \right]_{\alpha\beta} \quad (4)$$

with

$$\chi_{\alpha\beta}^{\text{irr}}(q) = -\frac{T}{N} \sum_k G_{\alpha\beta}(k+q) G_{\beta\alpha}(k). \quad (5)$$

Here we denote $q \equiv (\mathbf{q}, i\epsilon_l)$ with $\epsilon_l = 2\pi l T$ being the Matsubara frequency for bosons, and N the number of \mathbf{k} -points on a mesh.

With Dyson's equation,

$$[G(k)^{-1}]_{\alpha\beta} = [G^0(k)^{-1}]_{\alpha\beta} + \Sigma_{\alpha\beta}(k), \quad (6)$$

where G^0 is the bare Green's function $G_{\alpha\beta}^0(k) = [(i\omega_n + \mu - \epsilon_{\mathbf{k}}^0)^{-1}]_{\alpha\beta}$ with $\epsilon_{\mathbf{k}}^0$ the bare energy, we have solved the eqn.(3)-(6) self-consistently.

T_c may be obtained from Eliashberg's equation (for the spin-singlet pairing),

$$\lambda \phi_{\alpha\beta}(k) = -\frac{T}{N} \sum_{k'} \sum_{\alpha', \beta'} V_{\alpha\beta}^{(2)}(k-k') G_{\alpha\alpha'}(k') G_{\beta\beta'}(-k') \phi_{\alpha'\beta'}(k'), \quad (7)$$

where ϕ is the gap function, and the pairing interaction $V^{(2)}(k)$ is given as

$$V_{\alpha\beta}^{(2)}(q) = \frac{3}{2} U^2 \left[\frac{\chi^{\text{irr}}(q)}{1 - U\chi^{\text{irr}}(q)} \right]_{\alpha\beta} - \frac{1}{2} U^2 \left[\frac{\chi^{\text{irr}}(q)}{1 + U\chi^{\text{irr}}(q)} \right]_{\alpha\beta}. \quad (8)$$

T_c is determined as the temperature at which the maximum eigenvalue λ becomes unity.

The spin susceptibility,

$$\chi_{\alpha\beta}(\mathbf{k}, 0) = \left[\frac{\chi^{\text{irr}}(\mathbf{k}, 0)}{1 - U\chi^{\text{irr}}(\mathbf{k}, 0)} \right]_{\alpha\beta}, \quad (9)$$

may be expressed as diagonalized components,

$$\chi_{\pm} = \frac{\chi_{AA} + \chi_{BB}}{2} \pm \sqrt{\left[\frac{\chi_{AA} - \chi_{BB}}{2} \right]^2 + |\chi_{AB}|^2}. \quad (10)$$

Throughout this study, we take $N = 32^3$ k-point meshes, and the Matsubara frequencies taken from ϵ_n from $-(2N_c - 1)\pi T$ to $(2N_c - 1)\pi T$ with $N_c = 4096$, which give converged results.

III. RESULT

A. MgB₂

Let us first discuss the spin structure. We have fitted the shape of the Fermi surface to that obtained by the band calculation¹⁹ to have $t_z = 0.65, n = 1.03, U = 1.5$, and $T = 0.01$, where n is band filling ($n = 1$ for half filling). The Fermi surface, Fig.2, consists of two sets of tubular networks corresponding to the bonding and anti-bonding bands. The spin-susceptibility $\chi_+(\mathbf{k}, 0)$ displayed in the same figure shows a sharp peak around $(0, 0, \pi)$ reflecting a good nesting at $(0, 0, \pi)$.

Figure 3 shows the gap function obtained from Eliashberg's equation. The solutions having the largest λ are gapless ϕ_{d_1} and ϕ_{d_2} , which are degenerate. As expected from Kuroki-Arita¹⁸, a *gapful* ϕ_s does exist, although its λ is slightly smaller than that for the d-wave. We have called the former solutions 'd-wave' in that the gap function changes sign as $+-+-$ azimuthally (i.e., within each band), while the latter gap 's-wave' in that it does not. As a hallmark that the inter-band nesting is exploited in the (intra-band) pairing, all these solutions indeed have $\phi_{AA}(k)\phi_{BB}(k') < 0$. We can confirm in Eliashberg's eq.(7) that the sign change across the two bands works favorably to increase λ if we note $V_{\alpha\beta}^{(2)}(k - k') > 0$ (dominant at around $\mathbf{k} - \mathbf{k}' = (0, 0, \pi)$) and a relation for multiband Green's function $G_{\alpha\beta}(-k) = G_{\alpha\beta}^*(-k)$ which gives $G_{AB}(k')G_{AB}^*(-k') > 0$.

The fact that the dominant 'd-wave' solutions are doubly degenerate can be understood by a group theoretical argument²⁸, and these solutions belong to Γ_6^+ representation for the honeycomb system (while 's-wave' to Γ_1^+). The true gap function below T_c to maximize the gap, should be a linear combination of the two d-waves, $\phi_{d_1} + i\phi_{d_2}$, which breaks the time-reversal symmetry. This combination has *point nodes* on the Fermi surface, which is curious but natural as evident from Fig.4 that superposes two sets of nodal planes, which shows how the nodal planes intersect each other along some lines for the doubly degenerate function and how these lines in turn intersect the closed Fermi surface.

The reason why 's-wave' is only subdominant may be traced back to the Fermi surface, which is rather extended in \mathbf{k} space in this particular case, so that there

is an appreciable contribution from the intra-band pair scattering that the d-wave can exploit.

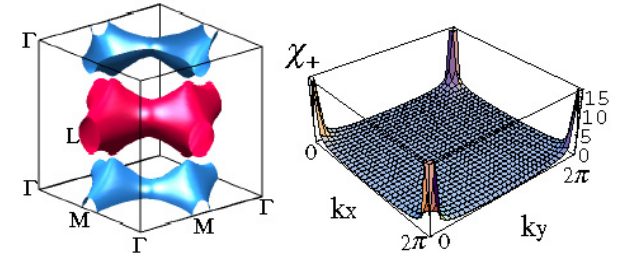


FIG. 2. Fermi surface (left panel, blue: bonding band, red: anti-bonding band) and χ_+ (right panel) with $k_z = \pi$ for $U = 1.5, n = 1.03, t_z = 0.65, T = 0.01$.

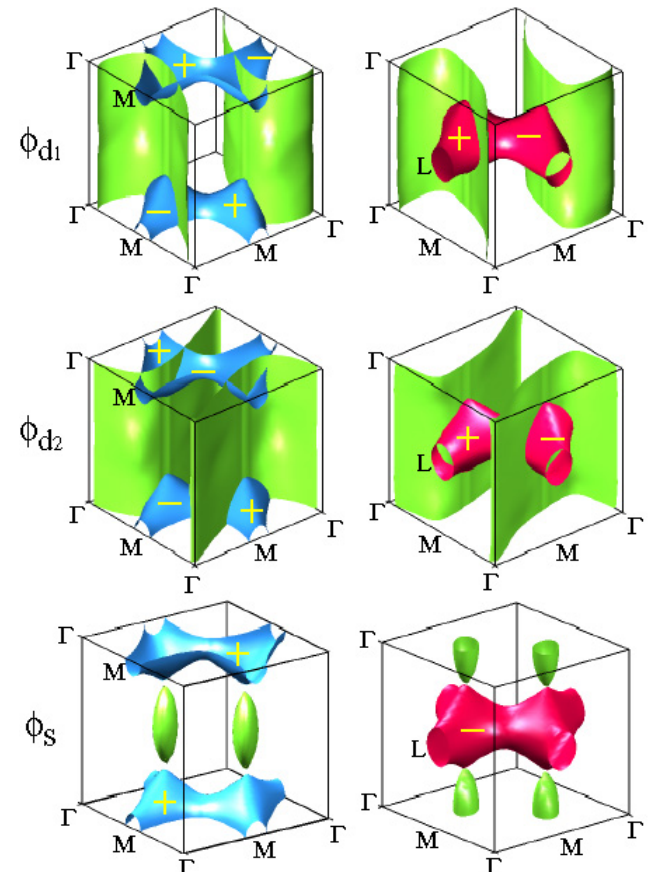


FIG. 3. The sign of the gap functions ϕ_{d_1} (top), ϕ_{d_2} (middle), and ϕ_s (bottom) for $U = 1.5, n = 1.03, t_z = 0.65, T = 0.01$. We have displayed the sign of the gap on the Fermi surface (left panels: bonding band, right panels: anti-bonding band) along with the nodal planes displayed in green.

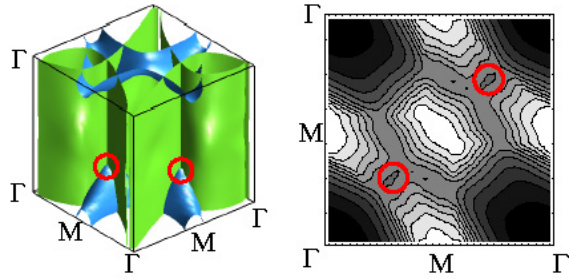


FIG. 4. Left panel superposes ϕ_{d_1} and ϕ_{d_2} for the bonding band. Right panel plots $|\phi_{d_1} + i\phi_{d_2}|$ for $k_z = 0$. The red circles denote point nodes in $\phi_{d_1} + i\phi_{d_2}$.

If we turn to the temperature dependence of λ in Fig.5, we can see that λ is significantly smaller than unity even for $T \rightarrow 0.01|t|$. This implies that the spin fluctuation alone is not strong enough to realize the d-wave superconductivity in this temperature range for the band filling and t_z taken here. On the other hand, the λ for the gapful ‘s-wave’ pairing is seen to have nearly the same magnitude as that of the gapless d-wave, although λ is again small. So the electron correlation can, thanks to the absence of nodes on the Fermi surface, give rise to a gapful pairing, which is eligible for assisting the phonon-mediated pairing if the electron-phonon interaction is considered on top of the electron-electron interaction²⁹. So we can conclude that inter-band spin fluctuations can work cooperatively with intra-band phonons to realize a gapful superconductivity.

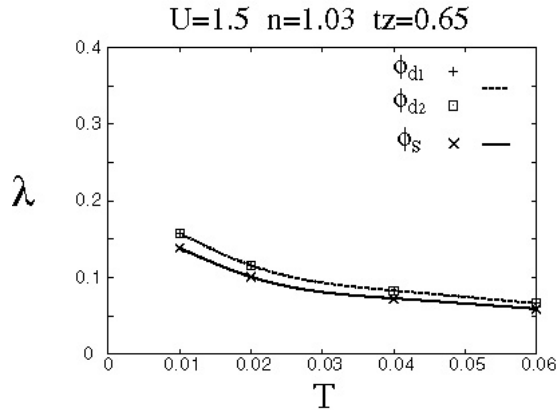


FIG. 5. The eigenvalue of Eliashberg’s equation λ versus temperature. The largest solutions are doubly degenerate. Lines in this and following figures are guide to the eye.

B. Optimization for the 3D honeycomb lattice

Let us move on to the strong coupling regime in search of superconductivity from electron repulsion alone. In general, pairing instability mediated by spin fluctuations in 3D systems is definitely weaker than that in 2D systems^{17,30}. This has been shown in a FLEX study for

the Hubbard model by three of the present authors, who have identified its reason in the k space volume fraction of the effectively attractive pair scattering region that is much smaller in 3D than in 2D.¹⁷ Furthermore, 3D systems have strong tendencies toward various magnetic orders, so that to identify the 3D systems that favor superconductivity from electron repulsion becomes a challenging problem.

Here we have optimized the pairing instability in the layered honeycomb lattice by varying the inter-layer hopping t_z and the band filling n . Namely, we have searched for sets of parameter values that give large values of λ without encountering antiferromagnetic instability at low temperatures. The resulting best parameter set is found to be $U = 8, n = 1.15, t_z = 0.7$ (inset of Fig.6), for which the Fermi surface and the spin susceptibility are shown in Fig.6. In Fig.7 we can see that the estimated $T_c \sim 0.001$ ($\lambda_{\max} \rightarrow 1$). The pairing symmetry is again $\phi_{d_1} + i\phi_{d_2}$.

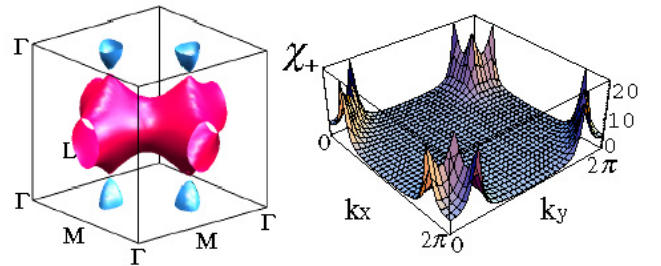


FIG. 6. Fermi surface (left) and $\chi_+(k_z = \pi)$ (right) for the optimized parameter set of $U = 8, n = 1.15, t_z = 0.7$ at $T = 0.01$, where the pairing symmetry is d-wave.

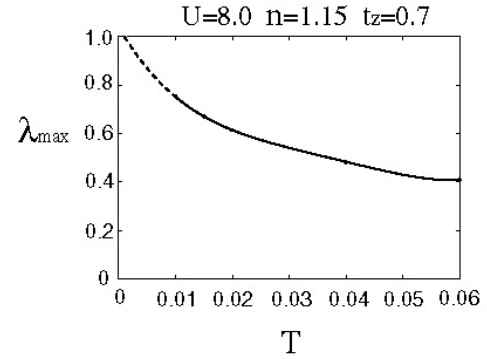


FIG. 7. λ versus temperature for the optimized parameter set employed in the previous figure. Dotted line is a spline extrapolation to lower temperatures.

C. Effect of the inter-band nesting

Apart from the above optimization, we have systematically explored how the inter-band nesting affects the

pairing in the 3D honeycomb lattice. Since we wish to separate out the effect of the band filling and the hopping in the z direction, we have done this along two paths displayed in Fig.8. The first path starts from the parameter values corresponding to the $p\pi$ bands in MgB_2 , while the second path includes the parameter regime ($t_z < 0.2$) which corresponds to GIC except for the value of U . The result along the first path is shown in Fig.9, where the n -dependence of λ_{\max} is plotted for $U = 1.5, t_z = 0.65$ at $T = 0.01$. We can see that the pairing instability becomes weaker as n is increased, which is natural since the inter-band nesting becomes degraded along this path.

The result along the second path is displayed in Fig.10, where λ is plotted as a function of t_z for $n = 1.2, T = 0.01$. Here we have adopted a rather large $U = 8$, because we want to have sizeable λ over a wide range of t_z including the case of bad nesting. There, we have covered both the layered case ($t_z < 1$) and a quasi-1D case ($t_z > 1$). Note that the case of 3D ($t_z = 0.8$) is more advantageous than the case of 2D ($t_z = 0$), which indicates that inter-band 3D nesting is effective for increasing λ on the present path. As indicated in Fig.10, antiferromagnetism occurs (i.e., $\chi \rightarrow \infty$) when the inter-band nesting becomes too strong as $t_z \rightarrow 1$ both from below and from above.

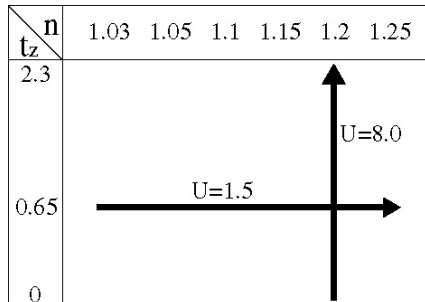


FIG. 8. The paths we have focused on in the present study in the parameter space of the inter-layer hopping t_z and the band filling n .

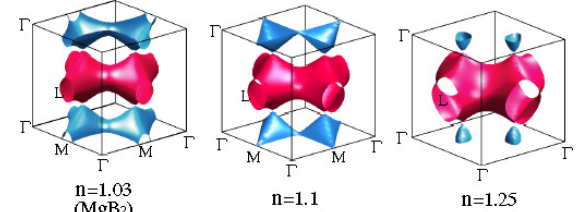
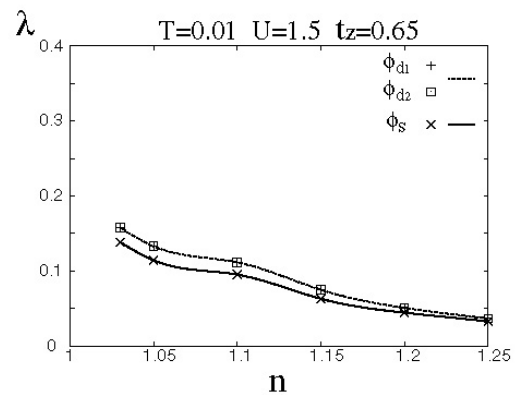


FIG. 9. λ versus n for $U = 1.5, t_z = 0.65, T = 0.01$. The d -wave solutions having the largest λ are doubly degenerate.

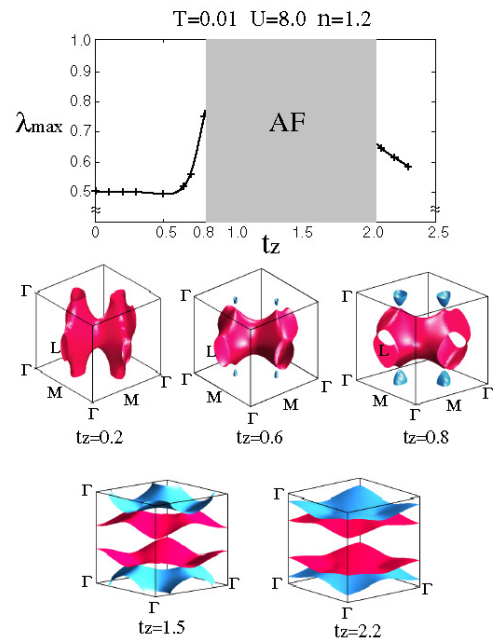


FIG. 10. λ versus t_z for $U = 8, n = 1.2, T = 0.01$. AF indicates the region for antiferromagnetism. The insets depict the shape of Fermi surface at five points on the horizontal axis.

IV. CONCLUSION

In conclusion, we have studied the possibility of spin-fluctuation mediated superconductivity in 3D honeycomb lattice systematically. We have shown that if we

take the parameter set which corresponds to the $p\pi$ bands in MgB₂, the spin fluctuation favors the gapful pairing, which suggests that the electron correlation can help the phonon to mediate the electron pairing. When strong enough, the electron repulsion alone will give rise to a d -wave pairing, with a time-reversal broken $\phi_{d_1} + i\phi_{d_2}$ symmetry associated with degenerate Γ_6^+ representations with point nodes on the Fermi surface.

V. ACKNOWLEDGEMENTS

Numerical calculations were performed at the Computer Center and the ISSP Supercomputer Center of University of Tokyo. This study is in part supported by a Grant-in-Aid for Scientific Research from the Ministry of Education of Japan.

¹ J. Nagamatsu, N. Nakagawa, T. Muranaka, Y. Zenitani, and J. Akimitsu, *Nature*, **410**, 63 (2001).

² N. A. W. Holzwarth, S. Rabii, and L. A. Girifalco, *Phys. Rev. B* **18**, 5190 (1978).

³ T. Inoshita, K. Nakao, and H. Kamimura, *J. Phys. Soc. Jpn.* **43**, 1237 (1977).

⁴ D. P. DiVincenzo and S. Rabii, *Phys. Rev. B* **25**, 4110 (1982).

⁵ J. H. Schön, C. Kloc, and B. Batlogg, *Science*, **293**, 2432 (2001).

⁶ H. J. Choi, D. Roundy, H. Sun, M. L. Cohen, and S. G. Louie, *cond-mat/0111182* (2001).

⁷ D. G. Hinks, H. Claus, and J. D. Jorgensen, *Nature*, **411**, 457 (2001).

⁸ S. L. Bud'ko, G. Lapertot, C. Petrovic, C. E. Cunningham, N. Anderson, and P. C. Canfield, *Phys. Rev. Lett.* **86**, 1877 (2001).

⁹ Y. Wang, T. Plackowski, and A. Junod, *Physica C* **355**, 179 (2001).

¹⁰ F. Bouquet, R. A. Fisher, N. E. Phillips, D. G. Hinks, and J. D. Jorgensen, *Phys. Rev. Lett.* **87**, 047001 (2001).

¹¹ T. Takahashi, T. Sato, S. Souma, T. Muranaka, and J. Akimitsu, *Phys. Rev. Lett.* **86**, 4915 (2001).

¹² S. Tsuda, T. Yokoya, T. Kiss, Y. Takano, K. Togano, H. Kitou, H. Ihara, and S. Shin, *cond-mat/0104489* (2001).

¹³ G. Karapetrov, M. Iavarone, W. K. Kwok, G. W. Crabtree, and D. G. Hinks, *Phys. Rev. Lett.* **86**, 4374 (2001).

¹⁴ P. Szabó, P. Samuely, J. Kačmarčík, T. Klein, J. Marcus, D. Fruchart, S. Miraglia, C. Marcenat, and A. G. M. Jansen, *Phys. Rev. Lett.* **87**, 137005 (2001).

¹⁵ F. Manzano, A. Carrington, and N. E. Hussey, *cond-mat/0110109* (2001).

¹⁶ X. K. Chen, M. J. Konstantinović, and J. C. Irwin, D. D. Lawrie, and J. P. Franck, *Phys. Rev. Lett.* **87**, 157002 (2001).

¹⁷ R. Arita, K. Kuroki and H. Aoki, *J. Phys. Soc. Jpn.* **69**, 1181 (2000); *Phys. Rev. B* **60**, 14585 (1999).

¹⁸ K. Kuroki, and R. Arita, *Phys. Rev. B* **64**, 024501 (2001).

¹⁹ J. Kortus, I. I. Mazin, K. D. Belashchenko, V. P. Antropov, and L.L.Boyer, *Phys. Rev. Lett.* **86**, 4656 (2001).

²⁰ K. Yamaji, *J. Phys. Soc. Jpn.* **70**, 1476 (2001).

²¹ N. Furukawa, *J. Phys. Soc. Jpn.* **70**, 1483 (2001).

²² N. E. Bickers, D. J. Scalapino, and S. R. White, *Phys. Rev. Lett.* **62**, 961 (1989).

²³ N. E. Bickers and D. J. Scalapino, *Ann. Phys. (N.Y.)* **193**, 206 (1989).

²⁴ T. Dahm and L. Tewordt, *Phys. Rev. B* **52**, 1297 (1995).

²⁵ M. Langer, J. Schmalian, S. Grabowski, and K. H. Bennemann, *Phys. Rev. Lett.* **75**, 4508 (1995).

²⁶ S. Koikegami, S. Fujimoto, and K. Yamada, *J. Phys. Soc. Jpn.* **66**, 1438 (1997).

²⁷ H. Kontani and K. Ueda, *Phys. Rev. Lett.* **80**, 5619 (1998).

²⁸ M. Sigrist and K. Ueda, *Rev. Mod. Phys.* **63**, 239 (1991).

²⁹ Here, we assume that phonons have long wavelength, so that they mainly mediate attractive pair scattering *within* each Fermi surface.

³⁰ P. Monthoux and G. G. Lonzarich, *Phys. Rev. B* **59**, 14598 (1999).